The Implementation of Quasi-Oriented Rotor Field Control Algorithm for Induction Motor Traction Systems

Mihăiță Lincă*, Constantin Vlad Suru*, Mihaela Popescu*, Alexandru Bitoleanu* and Cristian Bratu*
* University of Craiova, Faculty of Electrical Engineering, Craiova, Romania, mlinca@em.ucv.ro, vsuru@em.ucv.ro, mpopescu@em.ucv.ro, a_bitoleanu@yahoo.com, cbratu@elth.ucv.ro

***Abstract* - A rotor field quasi-oriented control algorithm for drive systems equipped with a low cost DSP system has been implemented and experimentally validated in this paper. The system is designed for induction motor traction systems. The control algorithm implementation was done for a dSPACE DS1103 prototyping board in the Matlab Simulink environment. The control algorithm principle is based on the assumption that the current system is oriented by the rotor flux and the real flux follows the imposed value. Therefore, the rotor flux estimation is no longer necessary as well as the flux control loop. This makes the control algorithm suitable for low cost industrial DSP applications. The drawback is given by the fact that the current projections on the dq axes cannot be regulated, the current control being done by means of the current phasor magnitude. The control system implementation was validated with good results, in terms of current and speed regulation especially at variable mechanical load (such as track joints or switches), making this method suitable not only for low cost traction systems, but especially for railway vehicles.**

Cuvinte cheie: *control cu orientare după câmp, motor de inducție, sistem de tracțiune.*

Keywords: *field oriented control, induction motor, traction system.*

I. INTRODUCTION

The induction motor is the standard motor used in general modern electric drive systems [1]. The same is valid for electric traction systems used in modern electric vehicles and especially in high power railway systems [2]. As catenary fed vehicles are not power limited by the battery, the traction system power can be very large. For these traction systems the field oriented control is an advantageous choice as it offers high torque at low speed and high dynamic performance [3]. A particularity of traction systems is the use of the traction motor above the rated speed. In this regime, the field oriented control gives good performance, given the fact that it implies higher frequency of the motor currents [1]. This is important because high power drive systems imply relatively low switching frequency (which affects the performance of the control system). At the same time, the motor current relatively high frequency needs a fast and high computing power DSP to execute the control algorithm in real time. Because the rotor field oriented control requires high computation power, unavailable for standard industrial DSPs, the aim of this paper is the implementation of a simplified, quasi-oriented rotor field control algorithm on a dSPACE DS1103 prototyping board. The experimental validation of the implemented control algorithm was done on an experimental railway traction stand.

II. ROTOR FIELD QUASI-ORIENTED CONTROL ALGORITHM

For the rotor field oriented control the motor currents are expressed in the dq referential which rotates with the rotor flux [1-8]. To avoid the estimation of the flux, assuming that the current phasor is oriented and the real rotor flux correctly follows the imposed flux, the real time determination of the flux phasor can be avoided. Therefore, the flux control loop, which gives the magnetizing current on the d axis of the referential, can be also avoided. This can lead to an important simplification of the control algorithm, effective for drive systems that use less powerful DSPs [9].

The control algorithm for traction systems with simplified rotor field orientation (quasi-orientation) is synthetized in [9], where [8]:

- $R\omega$ - speed controller;
- $|I_m|$ - current magnitude computation block;
- R_i - current controller;
- VSI - voltage source inverter;
- ≋ - three phase sinusoidal control signal generator;
- f_2^* - slip frequency computation block.

The algorithm inputs are the imposed rotor flux and the imposed speed. For the given flux value, assuming as stated that the system is oriented, the value of the imposed magnetizing current is obtained [8][9]:

$$i_{sd} = \frac{1}{L_m} \cdot \left(\Psi_{rd} + T_r \cdot \frac{d\Psi_{rd}}{dt} \right), \tag{1}$$

where [8]:

- T_r - rotor circuit time constant:

$$T_r = \frac{L_r}{R_r} = \frac{L_m + L_{\sigma r}}{R_r}, \tag{2}$$

- L_m - magnetizing inductance;
- $L_{\sigma r}$ - rotor leakage inductance;
- R_r - rotor resistance.

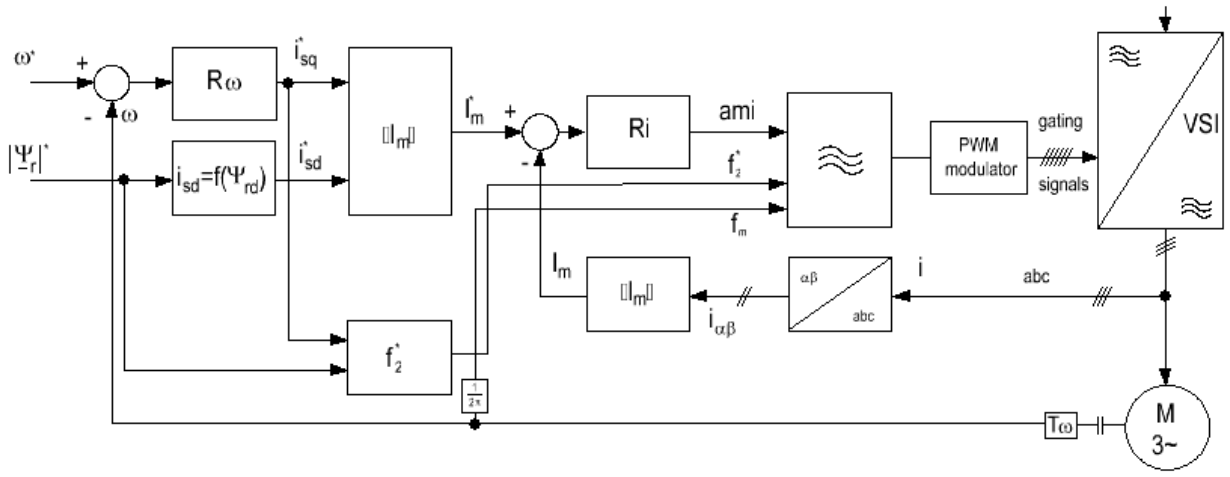

Fig. 1. Rotor field quasi-oriented control algorithm.

The imposed active current is obtained at the output of a proportional integrative speed controller [9].

The two currents are further used to compute the imposed motor current phasor magnitude (Fig. 1) used for the current control loop (which also uses a proportional integrative controller) [9]:

$$I_m^* = \sqrt{i_{sd}^2 + i_{sq}^2} \tag{3}$$

The feedback information is the real motor current phasor magnitude, computed from the measured three-phase currents [9]:

$$I_m = \sqrt{i_{s\alpha}^2 + i_{s\beta}^2} \tag{4}$$

where, i_α and $i_{s\beta}$, are the stator current phasor projections on the stationary reference frame [1], [6].

The output of the current magnitude controller is the amplitude modulation index ("ami" in Fig. 1) of the three phase sinusoidal control signals generated and applied to the PWM modulator. The frequency of these signals is obtained by summing to the motor shaft frequency, the imposed slip frequency [8]:

$$f_2^* = i_{sq} \cdot \frac{L_m}{2 \cdot \pi \cdot \Psi_{rd} \cdot T_r} \tag{5}$$

III. DS1103 Implementation of Rotor Field Quasi-Oriented Control Algorithm

The rotor field quasi oriented control algorithm was implemented for the experimental traction system in the Matlab Simulink environment. This was possible because the control subsystem of the traction system is made entirely by the dSpace DS1103 prototyping board, which can be programmed using this graphical programming environment. Of course, the experimental stand includes additional electronic circuits, but used only for auxiliary purposes (such as initialization, overcurrent/overvoltage protection, gate drivers, etc.), the control algorithm being completely implemented by the prototyping board.

Because the experimental stand is used to test a complete traction system it also includes the single phase rectified which feeds the traction inverter. It must be mentioned that the rectifier (which is a PWM boost rectifier) is not controlled by the prototyping board, but by a dedicated DSP (as it does not make the object of this study).

As illustrated in the prototyping board control model (Fig. 2), the control algorithm (Fig. 3) is grouped into a subsystem, for better clarity.

The link between the power system and the control algorithm (model) is done by the power section transducers (voltage, current and speed) and the DS1103 acquisition system. Each analog to digital converter (connected to a transducer) have a corresponding Simulink block (from the Real Time Interface library) which outputs a Simulink signal, further de-normalized (with the appropriate Gain blocks). Some of the converted signals are not needed for the control algorithm, but only for system monitoring purposes.

The speed transducer which was used is an incremental encoder therefore it was connected to the DS1103 incremental encoder specialized input. This gives at the output port of DS1103ENC_POS_C1 the number of increments further used to obtain the speed. Because of the relatively low number of pulses, the sliding window averaging technique was used to smooth the speed.

The output of the control algorithm (the IGBT gating signals) are obtained by applying the three phase generated control signals to the DS1103 hardware PWM modulator (by means of the DS1103SL_DSP_PWM3 block).

The actual control algorithm is illustrated in Fig. 3. It is also grouped in several subsystems for better understanding of the model, given the algorithm typical sections:

- The motor current magnitude – computed from the acquired three phase motor currents (in the αβ referential);
- The d axis (magnetizing) current obtained as a function of the imposed motor flux (for the assumption that the system is oriented);

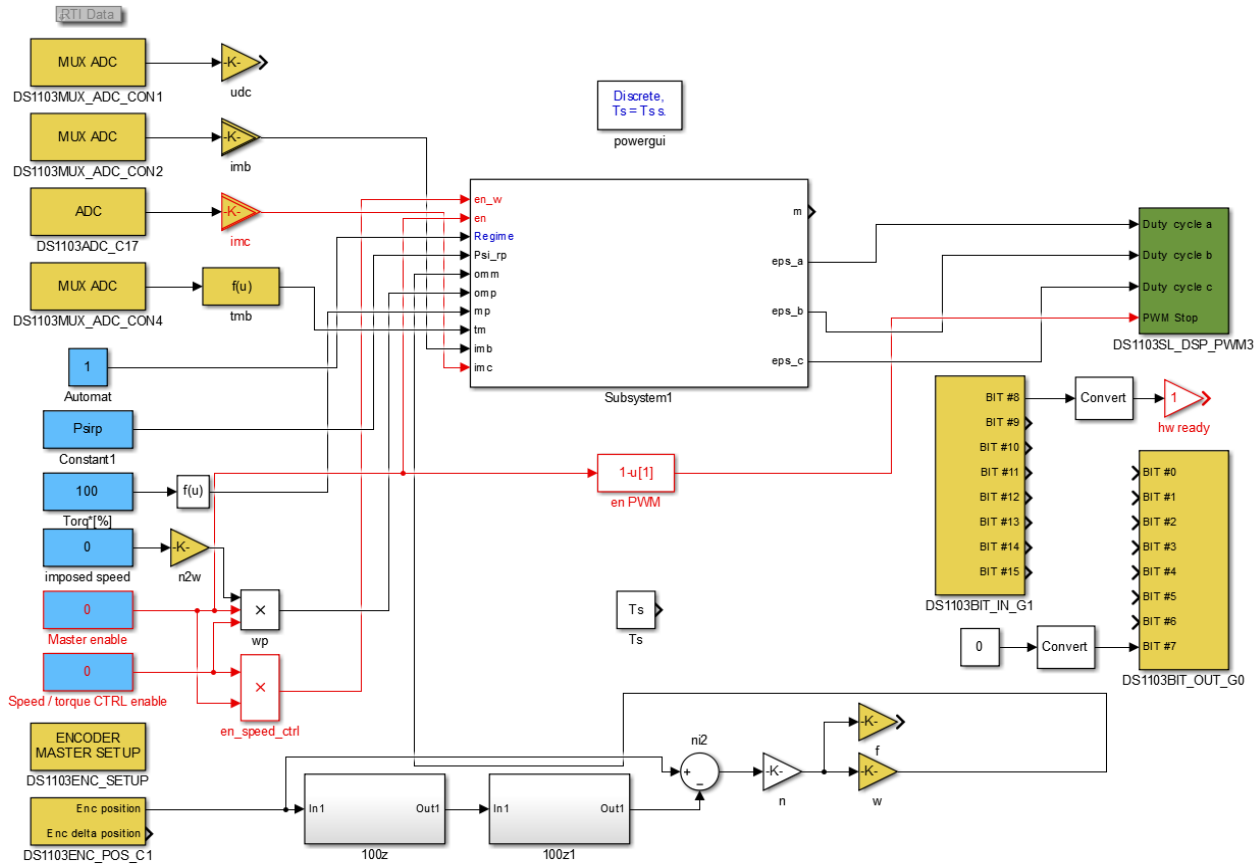

Fig. 2. The DS1103 Simulink control model.

- the slipping frequency, from the motor speed and motor equations;
- The imposed active stator current in the dq referential (i_{sq}).

The active current, i_{sq}, is imposed in two manners:

- Manual mode - the motor torque is directly imposed, from which the active current is computed.
- Automated mode – the active current is imposed at the output of the speed controller.

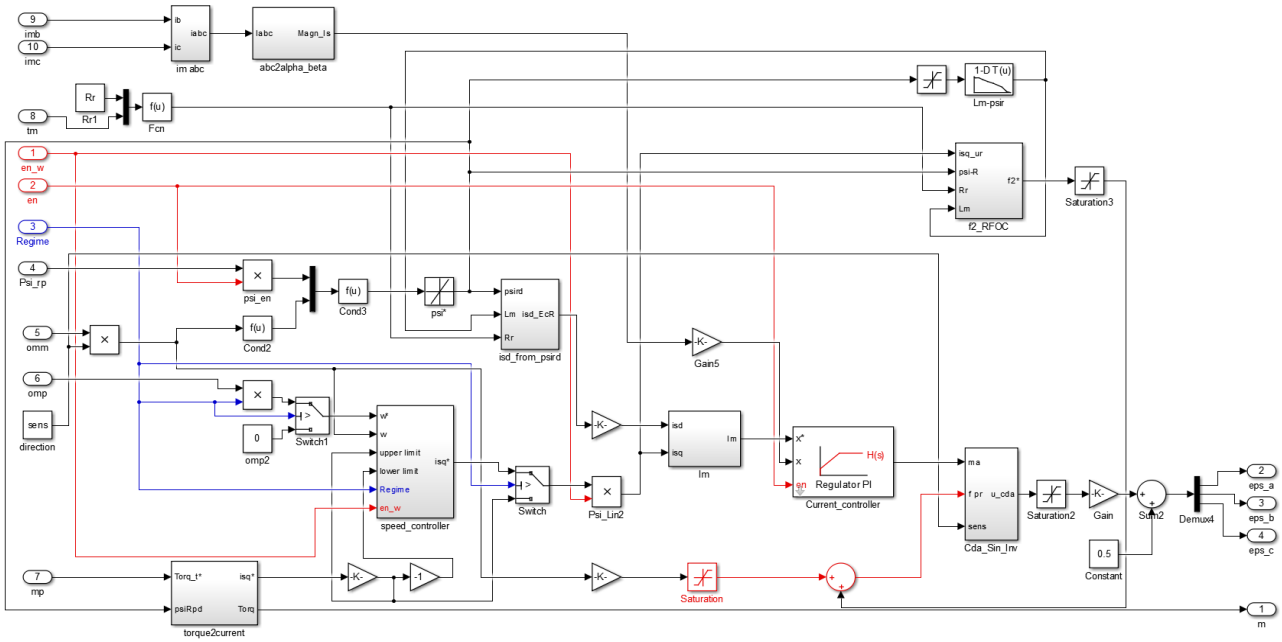

Fig. 3. The rotor field quasi-oriented control algorithm.

The q axis (active) current is obtained as a function of the imposed torque in the manual operating mode, and as the output of the speed controller, in the automated mode. For the latter, we still have the imposed torque, which in this case gives a corresponding current value which is further used to limit the speed controller output.

The two imposed currents are used to obtain the imposed current magnitude applied to the motor current magnitude controller. Its output is further applied as an amplitude modulation factor to the block which generates the three phase control signals. The frequency of the generated signals is obtained from the motor measured frequency by adding the slipping frequency.

Because the DS1103SL_DSP_PWM3 block (PWM modulator) accepts the duty factors for each inverter column, the three phase sinusoidal control signals are previously transformed to duty factors.

The real time control of the experimental traction system is done by means of a virtual control panel built in ControlDesk NG (which is the dSPACE specific control software) - Fig. 4 [11][12][13]**Error! Reference source not found.**. The control model blocks are linked to the virtual instruments of the control panel by means of block parameters or output signals [16][17]. The real time control is obtained by modifying block parameters (by the virtual instrument) and the output signals are used to monitor the system status and qualitative analysis of the system performance (by means of the virtual oscilloscopes). An important fact related to the virtual oscilloscopes (time plotters) for the analyzed case (Fig. 4) is that because of the extensive acquisition time length (25 s) the acquisition samples had to be decimated, therefore only part of the samples had been recorded (for the 100 μs sample time). This can lead to aliasing, for the periodic signals which is the case of the three phase control signals which seems to have low frequency at very high speed - Fig. 4. The same data illustrated on the time plotters of the control panel was also recorded, for offline analysis in Matlab [15][16][17].

IV. Experimental Setup

The DS1103 control system was embedded in a scale experimental traction system for railway vehicles composed of:

- Single phase PWM boost rectifier (controlled by local DSP);
- Three-phase inverter (controlled by DS1103);
- Three phase induction motor.

The rated parameters of the traction motor are:

- U_N = 380 V, I_N = 88 A, P_N = 50 kW;
- f_N = 65 Hz; n_N = 1917 rpm.

The mechanical load of the traction motor is a DC machine used as generator feeding a passive constant resistive load. Consequently, the traction motor mechanical load was controlled by means of the DC machine field current.

V. Experimental Results

The traction system performance was analyzed by accelerating the motor to twice the rated speed, simulating the railway joints.

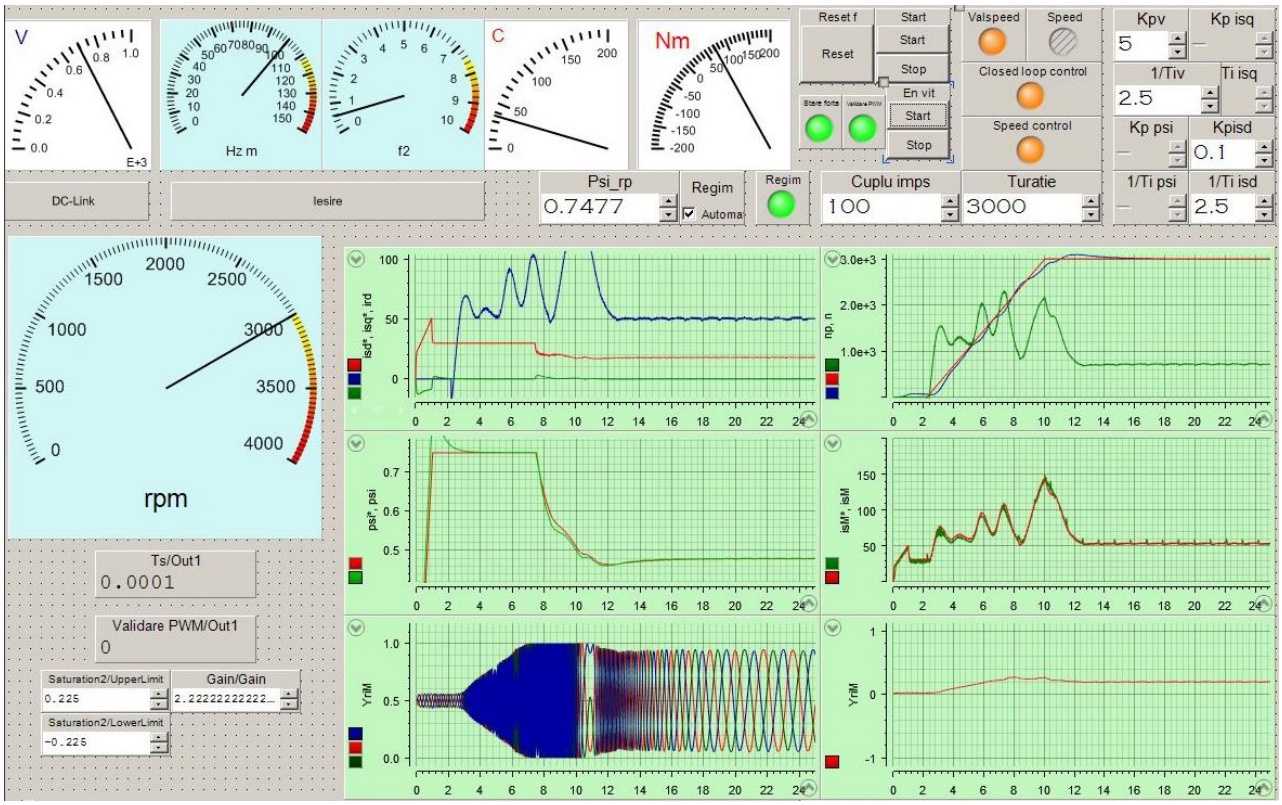

Fig. 4. The experimental system ControlDesk real time control panel.

The railway joints are the devices that connect two adjacent rails of the railway track. The passing of the wheel over the joint lead to high current transients due to the fact that the adjacent rails are not continuous but have an interstice necessary to allow their expansion. This means that the next rail the wheel is passing to can be slightly above or below the previous rail (with or without a gap). Depending on the position of the next rail (compared to the previous one) the torque at the traction motor shaft could have a steep increase or decrease leading to steep increase of the motor current or motor speed.

Not to exceed the DC machine rated power, the field current was set at 2 A (bellow the rated speed the field current can be increased up to 5A), but in order to simulate the railway joints, sudden, significant, positive or negative variations were imposed on it.

The evolution of the motor speed during the experiment is illustrated in Fig. 5. The traction motor was accelerated after the motor was magnetized. For this, the q axis component of the imposed motor phasor current magnitude was applied after the motor flux reached steady state operation (Fig. 6).

It can be seen that the speed is well regulated, with an overshoot of about 99 rpm (3.3% of the imposed speed). It must be taken into consideration that the motor accelerates under significantly variable load. Moreover, during the acceleration, a variation of the speed around the prescribed value can be observed, according to whether the static torque was positive or negative

Also, during magnetization, although the imposed speed is null (as well as the q axis imposed current) the real motor speed is not null (but about 68 rpm). This is because, in order to have sinusoidal magnetizing current at motor standstill, a minimum frequency of about 1.6 Hz was used. This gives a slow rotation of the motor shaft if the motor is idle. It must also be mentioned that during the magnetization the speed controller is inhibited, therefore the active current is null. Also, because the mechanical load is a DC generator, the motor is idle at standstill and no mechanical brake was applied.

The motor imposed flux is illustrated in Fig. 6. It can be seen that during magnetization, the flux increases linearly to its rated value and remains constant until the motor rated speed is reached. Above the rated speed the motor flux is weakened to avoid magnetic saturation. Because the flux weakening is done as a function of the real speed, the speed overshoot is "visible" on the imposed flux. This flux gives the imposed d axis current in Fig. 7.

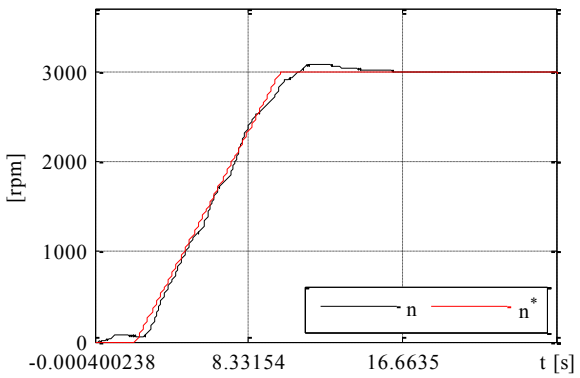

Fig. 5. The traction motor speed.

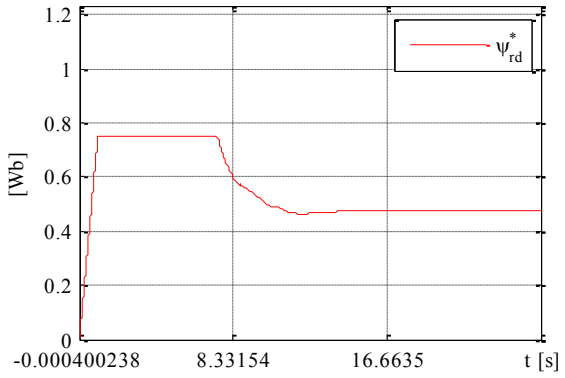

Fig. 6. The motor imposed flux.

Given the flux derivative in the magnetizing current expression, and as the flux depends on the actual speed (when weaken, above the motor rated speed), the speed variations are transmitted to the magnetizing current as seen in Fig. 7.

The active current is illustrated in Fig. 8. It can be seen that when the speed controller is activated, about 2.2 s after the motor magnetization had begun; the active current is initially negative, because of the motor slow rotation when magnetized. Subsequently it becomes positive as the imposed speed exceeds the real speed and the motor accelerates.

The imposed and real current are illustrated in Fig. 9. The torque variation (created by varying the DC machine field current) can be seen in the q axis imposed current shape, as the speed controller reacts to the steep variations of the mechanical load.

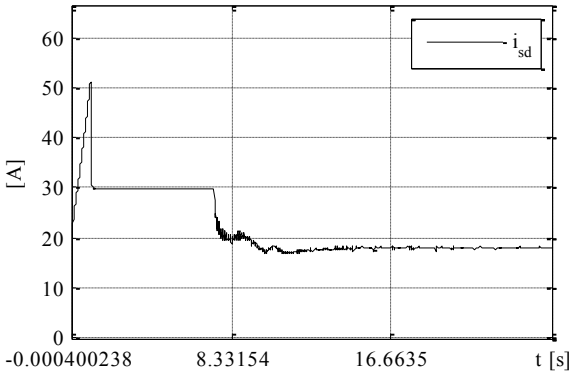

Fig. 7. The d axis imposed current.

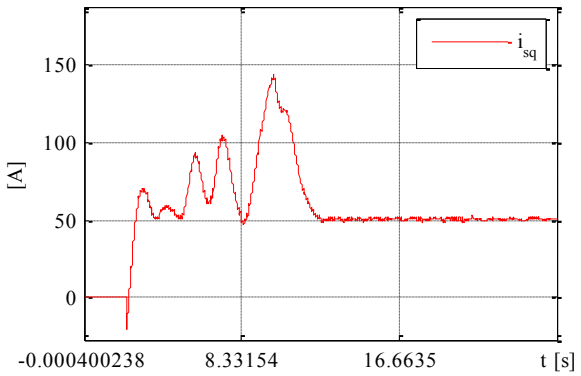

Fig. 8. The imposed q axis current.

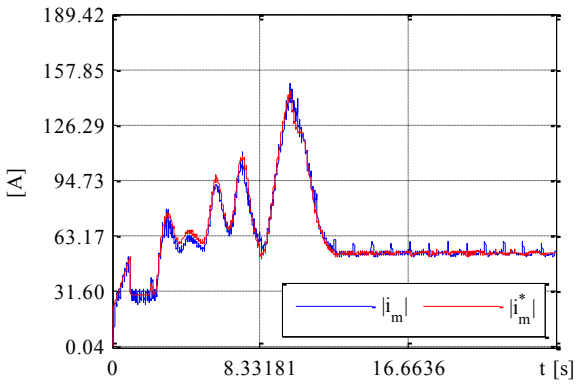

Fig. 9. The imposed and obtained motor current magnitude.

A small ripple can also be observed on the active current, but unlike the magnetizing current whose ripple appears only above the rated speed, the active current have ripple all the time (the speed controller is active). This is because the speed measured by the incremental encoder is not smooth (as the speed measured by a tachometer), but it has significant ripple, given by the limited number of pulses per revolution. Although it was greatly reduced by the two sliding window filters, the remaining ripple (amplified by the speed controller amplification (given by the proportionality constant) appears in the controller output, and consequently in the active current.

CONCLUSIONS

The rotor field quasi-oriented control algorithm for traction induction motors was experimentally implemented and validated in this paper. The obtained results proved the correct implementation of the control algorithm as well as the validity of the proposed system. Although the orientation of the system is only assumed and not really controlled, it gave good results both in static and dynamic regimes (in terms of current and speed regulation especially at variable mechanical load typical for railway vehicles such as track joints or switches). Driving the motor above the rated speed at weaken flux is also obtained with good results. The advantage of this control algorithm is given by the low computing resources required making it feasible for implementation on low cost control systems - the described experiments had been conducted with a time sample of 100 μs. The disadvantages of the proposed algorithm are given by the motor being unable to standstill when only magnetized (even with the speed controller inhibited, therefore, null active current). The motor speed is obtained by the slip frequency, but is null for null q axis current. In this situation it tends to rotate at low speed (if idle). This is because the motor magnetization is done with sinusoidal current, with a minimum frequency of 1.6 Hz, and the d axis current and q axis current cannot be controlled separately, but by means of the current magnitude. Although, this inconvenience appears only when the motor is idle, which is rarely met in practice as the railway vehicle is a considerable load itself. Moreover, it can be simply overcome by mechanically breaking the vehicle.

ACKNOWLEDGMENT

This work was supported by European Regional Development Fund, Competitiveness Operational Program, project PACETSINEFEN, ID: P_40_196/105687, (2016–2021).

Contribution of authors:

First author – 20%

First coauthor – 20%

Second coauthor – 20%

Fourth coauthor – 20%

Fifth coauthor – 20%

Received on September 9, 2024

Editorial Approval on November 29, 2024

REFERENCES

[1] A. M. Bazzi, A. P. Friedl, S. Choi and P. T. Krein, "Comparison of induction motor drives for electric vehicle applications: Dynamic performance and parameter sensitivity analyses," *2009 IEEE International Electric Machines and Drives Conference*, Miami, FL, USA, 2009, pp. 639-646, doi: 10.1109/IEMDC.2009.5075273.

[2] L. K. Jisha and A. A. Powly Thomas, "A comparative study on scalar and vector control of Induction motor drives," *International Conference on Circuits, Controls and Communications*, Bengaluru, India, 2013, pp. 1-5.

[3] T.C. Pană, O.C. Stoicuța, *Stability of Vector Drive Systems with Induction Motors* (*Stabilitatea sistemelor de acționare vectoriala cu motoare de inducție*), Cluj-Napoca: Mediamira, 2016.

[4] *Field Orientated Control of 3-Phase AC-Motors*, Literature Number: BPRA073, Texas Instruments Europe, February 1998.

[5] T. A. Wolbank, A. Moucka and J. L. Machl, "A comparative study of field-oriented and direct-torque control of induction motors reference to shaft-sensorless control at low and zero-speed," *Proceedings of the IEEE Internatinal Symposium on Intelligent Control*, Vancouver, BC, Canada, 2002, pp. 391-396, doi: 10.1109/ISIC.2002.1157795

[6] M. Popescu and A. Bitoleanu, "New achievements in the rotor field-oriented control for autonomous locomotives : Part 1: system synthesis and theoretical investigations," *2021 7th International Symposium on Electrical and Electronics Engineering (ISEEE)*, Galati, Romania, 2021, pp. 1-6.

[7] A. Bitoleanu, M. Popescu and V. Suru, "Experimental evaluation of rotor field orientation control and hysteresis controller for induction traction motor," *2021 12th International Symposium on Advanced Topics in Electrical Engineering (ATEE)*, Bucharest, Romania, 2021, pp. 1-6, doi: 10.1109/ATEE52255.2021.9425040.

[8] A Kelemen, M Imecs, *Sisteme de reglare cu orientare după cîmp ale mașinilor de curent alternativ*, Bucharest: Academiei, 1989.

[9] M. Linca, C. V. Suru, M. Popescu and A. Bitoleanu, "Rotor field quasi-oriented control algorithm implementation for railway traction systems on dSPACE DS1103," *2024 International Conference on Applied and Theoretical Electricity (ICATE)*, Craiova, Romania, 2024, pp. 1-6, doi: 10.1109/ICATE62934.2024.10748608.

[10] Real-Time Interface (RTI and RTI-MP) Implementation Guide for release 5.2, dSpace Gmbh, 2006.

[11] Simulink Coder – Target Language Compiler, © COPYRIGHT 2002–2017 by The MathWorks, Inc., www.mathworks.com

[12] Simulink Coder – User's Guide, © COPYRIGHT 2002–2017 by The MathWorks, Inc., www.mathworks.com

[13] Simulink Coder Reference, © COPYRIGHT 2002–2017 by The MathWorks, Inc., www.mathworks.com

[14] ControlDesk Next Generation Reference For ControlDesk 5.3, Release 2014‑B – November 2014.

[15] ControlDesk Next Generation Measurement and Recording Tutorial, For ControlDesk 5.3, Release 2014-B – November 2014.

[16] ControlDesk Next Generation Experiment Guide, For ControlDesk 5.3, Release 2014-B – November 2014.

[17] ControlDesk Experiment Guide, Release 2014-B – November 2014.